A Simulation Study of an Inverse Controller for Closed- and Semiclosed-Loop Control in Type 1 Diabetes

Agustín Rodríguez-Herrero, M.T.E.,[1,2] Carmen Pérez-Gandía, M.T.E.,[1,2] Mercedes Rigla, M.D., Ph.D.,[2,3] Alberto de Leiva, M.D., Ph.D.,[2,3] Enrique J. Gómez, Ph.D.,[1,2] and M. Elena Hernando, Ph.D.[1,2]

Abstract

Background: Closed-loop control algorithms in diabetes aim to calculate the optimum insulin delivery to maintain the patient in a normoglycemic state, taking the blood glucose level as the algorithm's main input. The major difficulties facing these algorithms when applied subcutaneously are insulin absorption time and delays in measurement of subcutaneous glucose with respect to the blood concentration.

Methods: This article presents an inverse controller (IC) obtained by inversion of an existing mathematical model and validated with synthetic patients simulated with a different model and is compared with a proportional-integral-derivative controller.

Results: Simulated results are presented for a mean patient and for a population of six simulated patients. The IC performance is analyzed for both full closed-loop and semiclosed-loop control. The IC is tested when initialized with the heuristic optimal gain, and it is compared with the performance when the initial gain is deviated from the optimal one (±10%).

Conclusions: The simulation results show the viability of using an IC for closed-loop diabetes control. The IC is able to achieve normoglycemia over long periods of time when the optimal gain is used (63% for the full closed-loop control, and it is increased to 96% for the semiclosed-loop control).

Introduction

In the last few decades a great research effort has been made in research in closed-loop diabetes control systems as a means of optimizing insulin therapy. Much work has been presented, but little of it has shown applicable results in subcutaneous use.[1] Advances in algorithm development, the versatility of insulin pumps, and increased reliability of continuous subcutaneous glucose sensors are the foundation for the short-term development of an ambulatory closed-loop control system.

The first electromechanical system meant to emulate pancreas function dates from 1974. Called Biostator, it was an experimental system for hospital use, using the intravenous route for measurement and intervention. The control algorithm was a proportional-integral-derivative (PID) and glucose feedback.[2]

For practical ambulatory interaction the intravenous route is not viable. Continuous glucose measurement and insulin administration require the subcutaneous route, which complicates control because of delays in both measurement and insulin action.[3,4] To cope with delays it is necessary to use control topologies such as feed-forward or semiclosed-loop control.[5,6] Research in the artificial pancreas field had been revitalized by the growing availability of continuous glucose sensors, although they still are not generally used in clinical practice because of their high cost, short life, and limited reliability.[7]

Some of the closed-loop techniques applied in diabetes include PID approximations,[8] model predictive control,[9,10] fuzzy control,[11] and robust control.[12] Semiclosed-loop control has been also evaluated as a means to reduce the peak postprandial glucose levels.[13] All the previous approaches provide unilateral control in which the hormone insulin is used to lower the glucose values, but there is no other counterregulatory mechanism. In a recent experiment, the hormone glucagon has been used in a closed-loop control system to prevent hypoglycemic episodes in pigs.[14]

This article presents an inverse controller (IC) for closed-loop and semiclosed-loop diabetes control based on an inversion model of the glucoregulatory system.[15]

[1]Bioengineering and Telemedicine Group, Polytechnic University of Madrid; and [2]Networking Research Centre for Bioengineering, Biomaterials and Nanomedicine, CIBER-BBN, Madrid, Spain.
[3]Endocrinology Service, Sant Pau Hospital, Barcelona, Spain.

Control by inversion is a technique that uses an inversion model to obtain infusion doses and also requires the availability of a glucoregulatory patient model. Various models have been proposed in the literature, from which we single out those of Bergman,[16] Guyton et al.,[17] Berger and Rodbard,[18] Gómez et al.,[19] Salzsieder et al.,[20] Lehmann and Deutsch,[21] Hovorka et al.,[22] and Dalla Man et al.[23]

Although a glucoregulatory inversion model has previously been used to obtain an estimation of plasma insulin,[24] it has not been used in closed-loop control. The proposed IC has been tested in silico with a simulated patient population and a glucose sensor model. Although in silico performance of a control algorithm does not guarantee in vivo performance, it helps to test extreme situations and the stability of the algorithm and to rule out inefficient scenarios.[25]

Methods

The glucoregulatory model

The controller design is based on the glucose dynamic model of Guyton et al.[17] and Lehmann and Deutsch,[21] modified by Gómez et al.,[19] and on the insulin dynamic described by Berger and Rodbard[18] adapted to the lispro type insulin.[26]

The glucose model[21] is a compartmental model whose parameters may be consulted in Table 1. The glucose balance equation is:

$$dG_{IV}(t)/dt = (G_{in}(t) - G_{out}(t) + G_{NHGB}(t) - G_{kid}(t))/V \quad (1)$$

where G_{IV} is the concentration of glucose in the blood, G_{in} is the glucose flow into the compartment due to the intestinal absorption of ingested carbohydrates (CHs), G_{out} is the peripheral consumption, G_{NHGB} is the hepatic balance, which can be positive or negative, G_{kid} is the renal excretion in hyperglycemic situations, and V is the dilution volume in the compartment.

CH absorption,[21] G_{in}, is calculated as:

$$G_{in}(t) = u_G(t)(e^{-r_1 t} - e^{-r_2 t}) r_1 r_2/(r_2 - r_1) \quad (2)$$

where u_G is the intake of CH (in g) and r_1 and r_2 are parameters defining CH type (Table 1).

Peripheral consumption,[17] G_{out}, is calculated as:

$$\begin{cases} K_x = (G_x + K_m)/G_x \\ G_{out-ID}(t) = K_x G_{IV}(t) c s_p I_{IV}(t)/(G_{IV}(t) + K_m) \\ G_{out-II}(t) = K_x G_{IV}(t) G_I/(G_{IV}(t) + K_m) \\ G_{out}(t) = G_{out-ID}(t) + G_{out-II}(t) \end{cases} \quad (3)$$

where $G_{out\text{-}ID}$ is the insulin-dependent glucose uptake, $G_{out\text{-}II}$ is the non–insulin-dependent glucose uptake, K_m is the Michaelis-Menten constant, G_x is the reference glucose level, c is the consumption ratio for insulinemia, I_{IV} is the plasma insulin concentration in equilibrium, s_p is the peripheral insulin sensitivity, and G_I is the insulin-independent glucose consumption.

Hepatic balance G_{NHGB} (glycogenesis and glycolysis) is modeled with the following equations obtained from experimental data[17]:

$$\begin{aligned} g_1(t) &= c_{11} - c_{12} \cdot G_{IV}^{c_{13}}(t)/(c_{14}^{c_{13}} + G_{IV}^{c_{13}}(t)) \\ g_2(t) &= c_{21} - c_{22} \cdot G_{IV}^{c_{23}}(t)/(c_{24}^{c_{23}} + G_{IV}^{c_{23}}(t)) \\ g_3(t) &= c_{31} + c_{32} \cdot G_{IV}^{c_{33}}(t) \cdot e^{-c_{34} \cdot G_{IV}^{c}(t)} \\ &\quad + c_{35} \cdot G_{IV}^{c_{36}}(t) \cdot e^{-c_{37} \cdot G_{IV}^{c}(t)} \\ G_{NHGB}(t) &= g_1(t) + g_2(t) \cdot e^{-g_3(t) I_{IV}(t) s_h/I_b} \end{aligned} \quad (4)$$

Table 1. IC Parameters

	Definition	*Value*	*Units*
I_b	Basal insulin	11	mU/L
K_e	1st-order constant for insulin elimination	5.4	H^{-1}
K_1	1st-order production active insulin	0.025	h^{-1}
K_2	1st-order removal active insulin	1.25	h^{-1}
a	Insulin-specific parameter (lispro)	0.02	h/U
b	Insulin-specific parameter (lispro)	1	H
s	Insulin-specific parameter (lispro)	1.7	h/U
T_{50}	Time for the half absorption of an insulin dose		H
G_x	Glycemic reference level	95	mg/dL
K_m	Michaelis-Menten constant	180	mg/dL
RTG	Threshold for kidney glucose elimination	160	mg/dL
GFR	Kidney glomerular filtration rate	1	dL/min
G_I	Glucose consumption independent from insulin	1.62	mg/min/kg
V	Dilution volume in the compartment	120	dL
W	Body weight	70	kg
r_1	CH absorption parameter		
	Fast absorption	0.08	min^{-1}
	Low absorption	0.017	min^{-1}
r_2	CH absorption parameter		
	Fast absorption	0.09	min^{-1}
	Low absorption	0.0173	min^{-1}
C	Peripheral glucose consumption dependent on the insulin concentration	0.045	mg L/min/kg/mU
S_p	Peripheral insulin sensitivity	0.5	
S_h	Hepatic insulin sensitivity	0.6	

where g_1 is the balance hepatic first component, g_2 is the linear hepatic coefficient, g_3 is the exponential hepatic coefficient (mmol/h), c_{ij} are adjustment parameters, and s_h is the hepatic insulin sensitivity.

Renal excretion (glycosuria),[17] G_{kid}, is calculated as:

$$G_{kid}(t) = \begin{cases} GFR(G_{IV}(t) - RTG)/M_G & G_{IV} > RTG \\ 0 & G_{IV} \le RTG \end{cases} \quad (5)$$

where GFR is the glomerular filtration rate and RTG is the renal threshold for glucose.

The insulin model[18] is composed of two compartments, which respectively model active insulin and insulin in equilibrium starting with the absorption of external insulin administered subcutaneously:

$$I_{abs}(t) = u_I(t) \cdot s t^s T_{50}^s / (t(T_{50}^s + t^s)^2) \quad (6)$$

where I_{abs} is the insulin absorbed, u_I is the insulin dosage, s is a specific parameter for each insulin type, and T_{50} is the absorption time of 50% of an insulin bolus:

$$dI(t)/dt = I_{abs}(t)/V - k_e I(t) \quad (7)$$

$$dI_a(t)/dt = k_1 I(t) - k_2 I_a(t) \quad (8)$$

where I_a and I are active and plasma insulin, respectively, k_1 and k_2 are insulin production constants, and k_e is an elimination constant.

When the blood insulin concentration is in equilibrium, $\hat{I}_{IV}$ is calculated as:

$$\hat{I}_{IV}(t) = (k_2/k_1) \sum_{n=0}^{N} I_{a,n}(t - t_n) \quad (9)$$

where N is the number of previously administered microboluses that still show activity at instant t, $I_{a,n}$ is the insulin due to the bolus n, and t_n is the administration time of bolus n.

The sensor model

The continuous glucose sensor was simulated with the intravenous-subcutaneous glucose dynamics defined by Facchinetti et al.[27] (see Eq. 10):

$$dG_{SC}(t)/dt = -(g/\tau)G_{SC}(t) + (1/\tau)G_{IV}(t) \quad (10)$$

where G_{SC} is the subcutaneous glucose, g and τ are parameters related to the transfer rate coefficients, and G_{IV} is the blood glucose.

Closed-loop control methodology

Figure 1 shows the topology of the IC in a full closed-loop IC (FCL-IC) configuration, which is composed of an inversor, a CH intake estimator, and an insulin dose calculator. The IC is a dual feedback controller. The main feedback is the controlled variable, the glucose continuous glucose monitoring (CGM), and the second feedback is the variable insulinemia.

The inversor. The inversor calculates the insulin in ideal equilibrium (I_{IVo}) that is required to neutralize CH intake disturbances. The inversor may be considered as an intravenous control strategy. The regulator has two inputs: the glucose measurement, G_{SC}, and an estimation of meal absorption, $\hat{G}_{in}$. The regulator output is I_{IVo}.[15]

The inversor is formulated through differential Eq. 1 under non-glycosuria conditions ($G_{kid} = 0$). The equation is discretized using a rectangular rule where T is the sample period:

$$G_{SC}(kT) - G_{SC}((k-1)T) = T(G_{in}(kT) - G_{out}(kT) + G_{NHGB}(kT))/V \quad (11)$$

The algorithm considers that in persons with type 1 diabetes, the ingested CHs ($\hat{G}_{in}$) are distributed as glucose used by the tissues (G_{out}) and glucose stored in the liver (G_{NHGB}) in a proportion of 50% each.[28]

The optimal insulinemia the patient should have in order to absorb the intake u_G is obtained through the inversion of Eqs. 3 and 4:

$$\begin{cases} G_{out-ID}(k) = 0.5\hat{G}_{in}(k) \\ G_{NHGB}(k) = -0.5\hat{G}_{in}(k) + G_{out-II}(k) \end{cases} \quad (12)$$

$$\begin{cases} I_{IVp}(k, G_{SC}) = 0.5\hat{G}_{in}(k) \cdot (G_{SC}(k) + K_m)/K_x G_{SC}(k) c \cdot s_p \\ I_{IVh}(k, G_{SC}) = -(I_b/g_3(k)s_h)\ln(-0.5\hat{G}_{in}(k) \\ \qquad + K_x G_{SC}(k) G_I/(G_{SC}(k) + K_m) - g_1(k))/g_2(k) \end{cases} \quad (13)$$

$$I_{IV}(k, G_{SC}) = I_{IVp}(k, G_{SC}) + I_{IVh}(k, G_{SC}) \quad (14)$$

where I_{IVp} and I_{IVh} are the concentrations of insulin required in the peripheral consumption and hepatic balance for correct intake absorption, respectively.

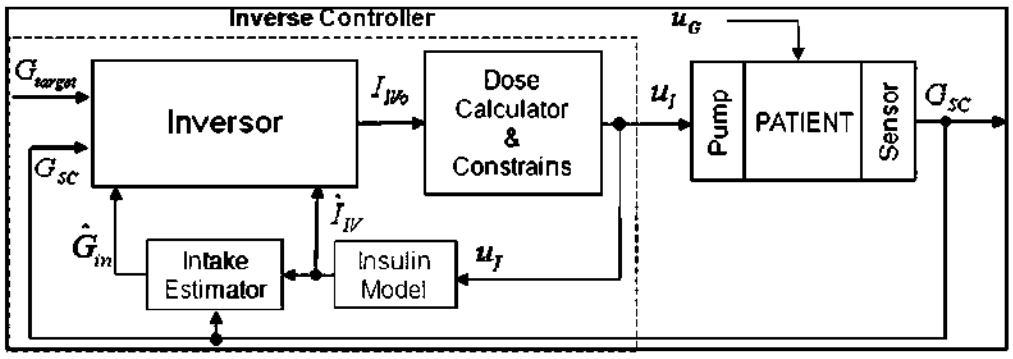

FIG. 1. Closed-loop subcutaneous IC and patient model. G_{target}, glucose target; $\hat{I}_{IV}$, insulinemia estimation; G_{SC}, subcutaneous glucose measurement; u_G, CH intake; $\hat{G}_{in}$, CH absorption estimation; I_{IVo}, optimum insulinemia; and u_I, insulin delivery.

The target insulinemia is calculated with Eq. 13 to reach the glucose target:

$$I_{\text{target}}(k, G_{\text{target}}) = I_{\text{IVp}}(k, G_{\text{target}}) + I_{\text{IVh}}(k, G_{\text{target}}) \quad (15)$$

The required insulin has to take into account the insulin that is already active in plasma from previous administration. Equations 14 and 15 calculate the incremental plasma insulin concentration:

$$\begin{cases} \Delta I_{\text{IV}}(k) = I_{\text{IV}}(k) - \hat{I}_{\text{IV}}(k) \\ \Delta I_{\text{target}}(k) = I_{\text{target}}(k) - \hat{I}_{\text{IV}}(k) \end{cases} \quad (16)$$

where I_{target} is the insulinemia required to reach the glucose target, I_{IV} is the insulinemia to absorb the intake, and $\hat{I}_{\text{IV}}$ is the equilibrium plasma insulin due to previous administrations.

The optimum insulinemia to achieve the target and to absorb the intake (I_{IVo}) is the sum of the two incremental terms in:

$$I_{\text{IVo}}(k) = I_{\text{target}}(k) + I_{\text{IV}}(k) - 2\hat{I}_{\text{IV}}(k) \quad (17)$$

The intake estimator. In an automatic regulator using glucose measurement as its only input, insulin starts to be administered once the effects of the intake appears in the glycemic levels, which means some minutes after the meal.

The proposed controller includes a CH absorption intake estimator that permits detection, at an early stage, of rising glucose and thus reduces as much as possible the time lapse between the meal and the start of insulin administration by the algorithm.

The intake estimator estimates the absorption of CHs by way of a new formulation of Eqs. 1–4:

$$\begin{aligned} \hat{G}_{\text{out}}(k) &= K_x G_{\text{SC}}(k)(cs_p \hat{I}_{\text{IV}}(k) + G_I)/(G_{\text{SC}}(k) + K_m) \\ \hat{G}_{\text{NHGB}}(k) &= \hat{g}_1(k, G_{\text{SC}}) + \hat{g}_2(k, G_{\text{SC}}) e^{-\hat{g}_3(k, G_{\text{SC}}) \hat{I}_{\text{IV}}(k) s_h / I_b} \\ \hat{G}_{\text{in}}(k) &= V(G_{\text{SC}}(k) - G_{\text{SC}}(k-1))/T + \hat{G}_{\text{out}}(k) - \hat{G}_{\text{NHGB}}(k) \end{aligned} \quad (18)$$

where $\hat{G}_{\text{out}}$ and $\hat{G}_{\text{NHGB}}$ are estimations of the patient's peripheral consumption and hepatic balance, respectively, G_{SC} is the subcutaneous glucose, $\hat{I}_{\text{IV}}$ is the insulinemia estimation, $\hat{g}_i$ is the estimation of the hepatic coefficients, and $\hat{G}_{\text{in}}$ is the estimation of CH absorption.

Dose calculator. Given that the inversor output is the plasma insulin concentration, the controller requires a method to calculate the insulin doses in order to obtain the optimal insulinemia in the least time possible, considering previously administered insulin and absorption delay. The dose calculator computes the required subcutaneous insulin pump infusions following the inversion concept and is based on the inversion of Eqs. 6–9:

$$\begin{aligned} u(k) &= K_u \sum_{i=0}^{2} q_i [d^i I_{\text{IVo}}(t)/dt^i]_{t=kT} \\ q_0 &= VK_e/f \\ q_1 &= V(1 + K_e/K_2)/f \\ q_2 &= V/(fK_2) \\ f &= s(kT)^s T_{50}^s / (kT(T_{50}^s + (kT)^s)^2) \end{aligned} \quad (19)$$

where u is the infusion dose, K_u is a gain adjusted to the patient, q_i are the terms resulting from the inversion, and I_{IVo} is the optimal insulinemia; f is a common term. The rest of the parameters are from Eqs. 1, 7, and 8.

Insulin dose constraints. To guarantee patient safety some constraints are applied to the calculated insulin doses:

- Null insulin microinfusions are not permitted except in the case of the onset of a hypoglycemic episode ($G_{\text{SC}} < G_{\text{off}}$), when insulin administration is suspended until glycemia reaches a safety threshold ($G_{\text{SC}} > G_{\text{on}}$). When the pump is suspended, a minimum pump dose (u_p) is administered every 60 min to avoid catheter occlusions.
- In the normoglycemic state, a minimum basal dose (u_b) is administered whenever the controller proposal falls below (u_b).
- To prevent postprandial hypoglycemic episodes, insulin infusion is limited to a maximum value calculated as follow: over the preceding 2 h, it will not exceed 30% of the total amount of daily insulin recommended for each patient.

Equation 20 shows the insulin dose constraints:

$$u_I = \begin{cases} u \begin{cases} G_{\text{SC}} > G_{\text{off}} \text{ if } u_I = u \\ G_{\text{SC}} > G_{\text{on}} \text{ if } u_I = u_b \end{cases} \\ 0 \text{ or } u_p \begin{cases} G_{\text{SC}} < G_{\text{off}} \text{ if } u_I = u \\ G_{\text{SC}} < G_{\text{on}} \text{ if } u_I = u_b \end{cases} \\ u_b \ u(k) \le u_b \\ u_m \ u(k) \ge u_m \end{cases} \quad (20)$$

where u_I is the controller-computed insulin dose, G_{SC} is the subcutaneous glucose, u_p is the smallest pump bolus, G_{off} is the hypoglycemic safety threshold, G_{on} is the activation threshold, u_b is the basal bolus, and u_m is the maximal bolus.

Semiclosed-loop control methodologies

The use of a semiclosed-loop IC (SCL-IC) approach could minimize the harmful effects of the delays. In a semiclosed-loop scenario the patient should provide to the algorithm information about the meals both in time and in CH content. The insulin bolus can be calculated with a personalized CH to insulin ratio. In this work, a percentage of the insulin bolus is administered prior to the meal, so the insulinemia starts to increase before the rise in the subcutaneous glucose measurement.

Simulation studies

The objective is to analyze in silico the impact of the FCL-IC on glucose control and the further improvement that can be obtained with an SCL-IC.

The patient population was simulated using the compartmental model defined by Hovorka et al.[22] and the six patients (numbers 1–6) identified by use of a dual-tracer dilution methodology. For single patient studies, we used the mean patient for the same population (patient number 0).[22]

The same meal plan is established for all the simulated patients: 205 g/day CH divided into five intakes (45 g at breakfast, 7 a.m.; 70 g at lunch, noon; 5 g at snack, 4 p.m.; 80 g at dinner, 6 p.m.; and 5 g at snack, 11 p.m.).[23]

The IC is applied to the simulated population using the following common parameters: Target = 100 mg/dL; G_{off} = 100 mg/dL; G_{on} = 105 mg/dL; u_b = 0.05 IU; u_p = 0.05 IU; u_{max} = 5 IU; g = 0.92; τ = 19.52 min.

The initial gain value (K_u) was heuristically adjusted for each patient and for each control mode (FCL-IC or SCL-IC) to obtain an optimal glucose profile in the range of 70–180 mg/dL while trying to avoid hypoglycemic events when using the controller. The SCL-IC administers 50% of the insulin bolus 15 min in advance of the announced meal.

The performance of the IC is analyzed when running with the heuristic optimal gain and is compared with the performance when the initial gain is deviated from the heuristic one (±10%).

FCL-IC insulin delivery is compared with the insulin delivered by a PID controller similar to that defined by Steil et al.[8] (it has been initialized with K_p = 0.001, T_i = 450 min, and T_d = 66 min), but applying, in addition, the insulin dose constraints defined in this work (pump suspension when $G_{SC} < G_{off}$, minimum pump dose, etc.). In both cases, the sample measurement period and insulin infusion period are 5 min long.

In the previous simulations, the sensor model[27] considered the plasma interstitial lag, but not the presence of noise in the measurement. To assume a white noise across the whole spectrum is generally inaccurate.[29] Therefore, in order to understand the impact of real noise on the IC, a CGM profile is used as input to the controller. The CGM data are from a patient wearing the Guardian® RT CGM System (Medtronic-Minimed, Northridge, CA) for 3 days. The input to the controller is the sensor data without any filtering process. We point out that, in this case, insulin therapy was open loop, so the glucose profile was retrospectively used as IC input, but the IC output (insulin administration) was not applied to the patient.

Results

Figure 2 shows a 2-day simulation for the FCL-IC and SCL-IC when applied to simulated Patient number 0 (the mean patient[22]). The upper graphs display the insulin infusion, and the lower graphs display the subcutaneous glucose concentration. The FCL-IC has been initialized with $K_u = 3.3\times10^{-3}$. The SCL-IC has been initialized with $K_u = 2.4\times10^{-3}$, and the prandial insulin bolus is administered 15 min before the meal. Table 2 summarizes the results presented in Figure 2: average daily insulin; the maximum, minimum, and mean glucose values; the number of glucose samples above and below the target range (70–180 mg/dL); and the area under the curve (AUC) above 180 mg/dL.

Figure 3 shows a 2-day simulation for the FCL-IC and SCL-IC when applied to the simulated population (without patient number 0). The graphs display the average glucose profile and the dispersion (mean ± SD) for the optimal gain (K_u), an over-dimensioned gain (K_u +10%), and an under-dimensioned gain (K_u −10%). Table 3 summarizes the results presented in Figure 3: maximum, minimum, and mean glucose values; the number of samples above and below the target range (70–180 mg/dL); and the AUC above 180 mg/dL.

Figure 4 shows the comparison between FCL-IC insulin delivery and PID insulin delivery in a 2-day simulation for simulated patient number 0 (the mean patient). The upper

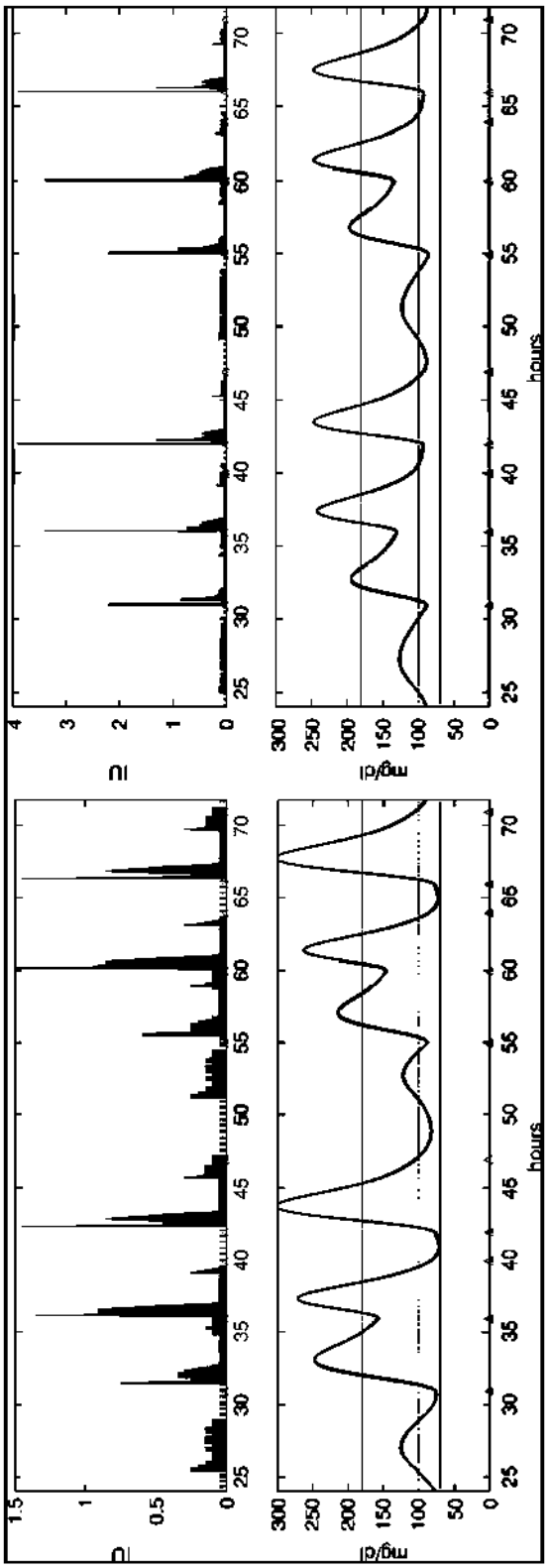

FIG. 2. Two days of simulation of the response of patient number 0 to the (**left**) FCL-IC and (**right**) the SCL-IC: (**upper graphs**) subcutaneous insulin infusion (u_{ll}) and (**lower graphs**) subcutaneous glucose concentration (G_{SC}). The triangles indicate the presence of a meal. Color images available online at www.liebertonline.com/dia.

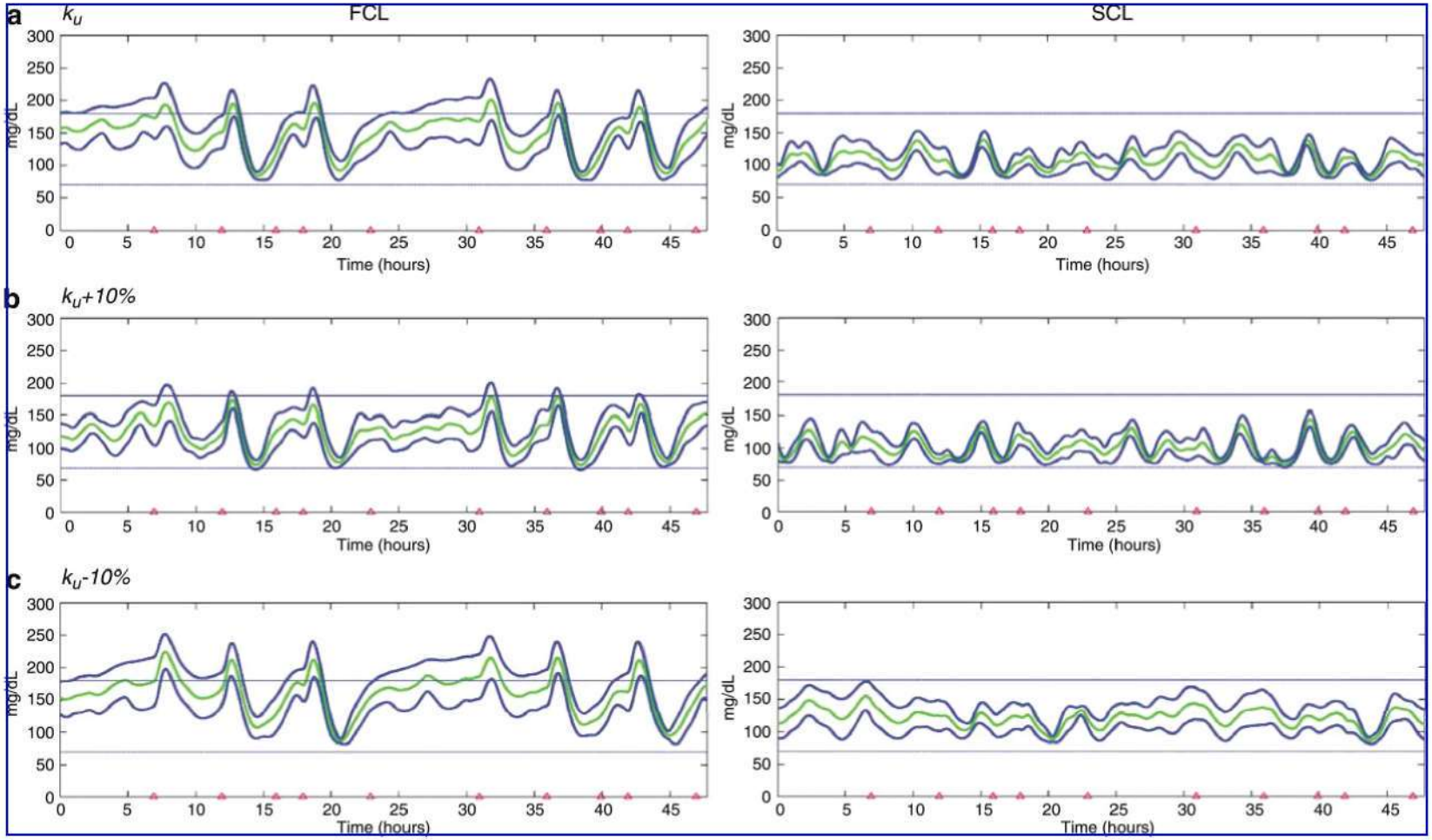

FIG. 3. Impact of the controller gain initialization (K_u) on the subcutaneous glucose concentration in the population of 2 days of simulation in response to (**left**) the FCL-IC and (**right**) the SCL-IC: (**a**) K_u = heuristically adjusted gain, (**b**) over-dimensional gain, and (**c**) under-dimensional gain. The triangles indicate the presence of a meal. Color images available online at www.liebertonline.com/dia.

Table 2. Results of the FCL-IC and SCL-IC Simulations for Patient Number 0

Gain, control mode	*Daily insulin (IU)*	*Glucose max/min (mg/dL)*	*Glucose (mean ± SD) (mg/dL)*	*% samples <70/>180 mg/dL*	*AUC > 180 (mg/dL/min)*
K_u +10%					
FCL-IC	39	304/56	136 ± 66	14/27	68
SCL-IC	41	223/62	115 ± 39	7/6	8
K_u					
FCL-IC	37	303/71	148 ± 64	0/30	80
SCL-IC	40	229/71	124 ± 39	0/11	12
K_u −10%					
FCL-IC	36	303/83	154 ± 58	0/83	78
SCL-IC	38	230/85	136 ± 38	0/16	19

graph displays FCL-IC insulin infusion, the middle graph displays PID insulin infusion, and the lower graph displays the subcutaneous glucose concentration. The numerical results with FCL-IC are presented in Table 2. The numerical results with PID are: daily insulin = 36.1 IU; $G_{max} = 317.5$ mg/dL; $G_{min} = 65.8$ mg/dL; $G_{mean \pm SD} = 161.4 \pm 70.2$ mg/dL; percentage of glucose samples below 70 mg/dL = 2.5%; percentage of glucose samples below 180 mg/dL = 36%; and AUC above 180 mg/dL = 69.

Figure 5 shows the SCL-IC response when a real CGM profile is used as input to the controller. The CGM data are from a patient wearing the Guardian RT CGM System. The upper graph shows the proposed subcutaneous insulin infusion, and the lower graph shows the subcutaneous glucose concentration. We point out that this simulation can help to understand the impact of noise on IC behavior, but, in this case, the real glucose profile is retrospectively used as IC input and the insulin was not delivered to the patient.

Conclusions

This work has shown the viability of utilizing an IC for closed-loop diabetes control in simulation studies. The IC is able to achieve normoglycemia over long periods of time when the optimal gain is used (63% for the FCL-IC but increased to 96% for the SCL-IC).

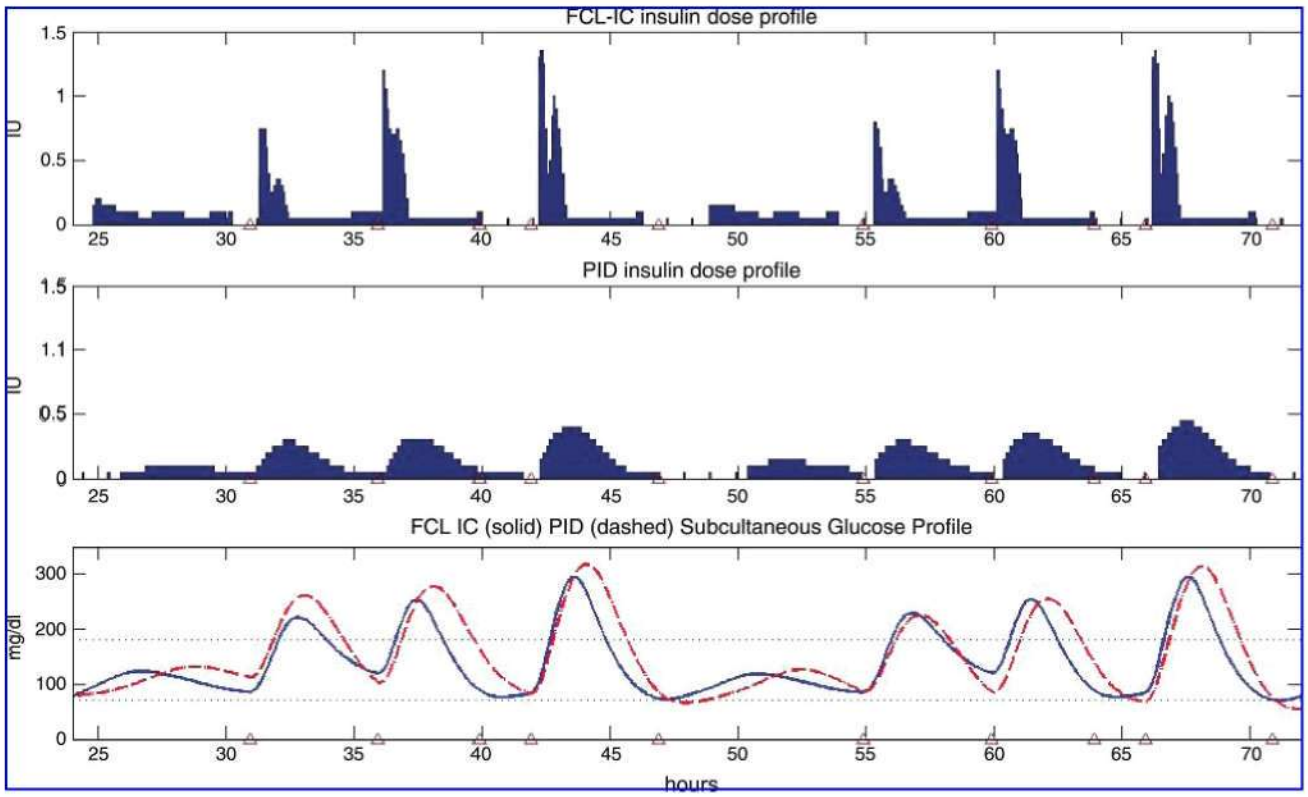

FIG. 4. Two days of simulation of the response of patient number 0 to the FCL-IC and the PID: (**upper graph**) FCL-IC insulin infusion, (**middle graph**) PID insulin infusion, and (**lower graph**) subcutaneous glucose infusion (solid line, FCL-IC; dashed line, PID). The triangles indicate the presence of a meal. Color images available online at www.liebertonline.com/dia.

TABLE 3. RESULTS OF THE FCL-IC AND SCL-IC SIMULATIONS FOR THE SIX-PATIENT POPULATION

Gain, control mode	*Glucose max/min (mg/dL)*	*Glucose (mean ± SD) (mg/dL)*	*% samples <70/>180 mg/dL*	*AUC > 180 mg/dL/min*
K_u +10%				
FCL-IC	266/58	125 ± 37	6/10	11
SCL-IC	195/55	101 ± 28	5/1	<1
K_u				
FCL-IC	288/70	147 ± 47	0/37	59
SCL-IC	229/71	108 ± 28	0/4	3
K_u −10%				
FCL-IC	306/73	160 ± 52	0/43	78
SCL-IC	239/72	122 ± 39	0/10	15

The proposed IC responds to a meal with a nonsymmetrical distribution of the insulin administered, with higher rates just after the intake than some minutes later. This nonlinear behavior helps to reduce the incidence of postprandial hyperglycemic episodes and cannot be observed in linear controllers such as the PID (see Fig. 4).

However, as observed by other authors, automated closed-loop controllers cannot achieve the glucose target after meals. Those postprandial hyperglycemic episodes cannot be avoided because of the delays introduced by subcutaneous measurement and subcutaneous insulin absorption. The results obtained with the simulated patient group show that the FCL-IC is able to achieve normoglycemia over long periods of time when the optimal heuristic K_u gain is used, but the performance of the algorithm decreases when the gain is not the optimal one. Table 3 shows that an over-dimensioned gain provokes hypoglycemic episodes (6%) and an under-dimensioned gain causes longer and more marked hyperglycemic episodes (43%), with an AUC of 78 mg/dL/min.

As expected, the semiclosed-loop approach is an improvement over full closed-loop glucose control as it is able to maintain normoglycemia over longer periods of time (96% vs. 63%). In additional, it is observed that the SCL-IC is more independent of a nonoptimal estimation of real subjects' parameters (controller gain): for all the gains considered, SCL-IC-related hypoglycemic events are similar to those observed with the FCL-IC, but the hyperglycemic episodes are reduced (Table 3). The reason is that a significant percentage of the insulin is administered manually before the meals and follows the patients' conventional daily therapy. The inconvenience of the SCL-IC is that it would require the patient to enter the mealtime and CH content into the controller. Thus, we lose the concept of an automated system, but it minimizes the effects of the delays.

The results show that both IC versions are protected against excessive insulin administration (over-dimensioned gains). This behavior is due to the insulin constraints that we have defined to avoid hypoglycemic events. It should be pointed out that the constraints are external to the controller and could be used in combination with any other control methods.

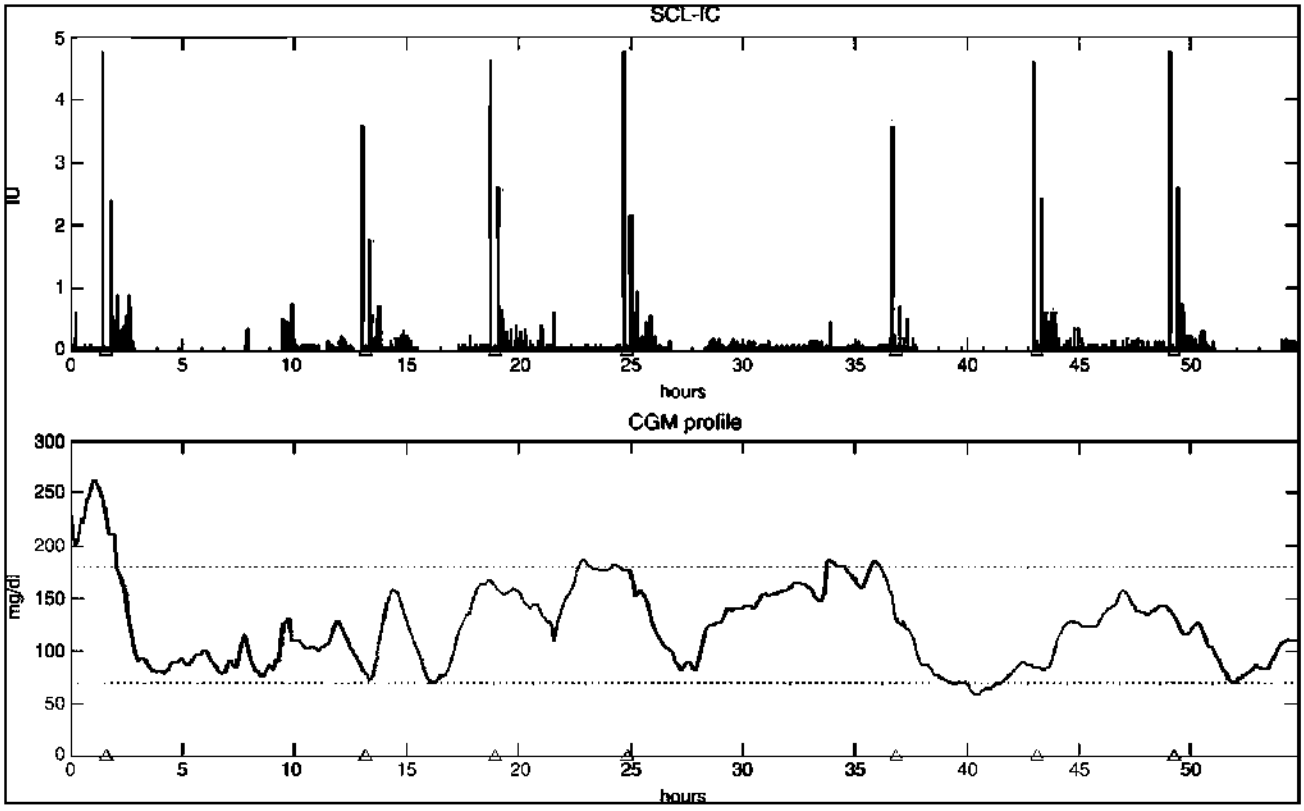

FIG. 5. Response of the SCL-IC when the input is a real CGM glucose profile: (**upper graph**) proposed subcutaneous insulin infusion and (**lower graph**) subcutaneous glucose concentration (measured with the Guardian RT). The triangles indicate the presence of a meal. Color images available online at www.liebertonline.com/dia.

As a first approach, the SCL-IC presented here administers 50% of the bolus before the meal and takes into account a fixed ratio of CH to insulin throughout the day. More in-depth studies should be carried out to assess the best approach.

The findings presented in Figure 4 suggest that the presence of noise in the glucose profile will degrade IC performance, resulting in a spurious insulin profile. A more in-depth analysis is required to characterize CGM sensor noise in order to simulate the impact on the IC.

Some keys that could improve any full closed-loop control are the development of adaptation mechanisms, the use of glucose prediction, the definition of different glucose targets over time, and the definition of initialization procedures. The use of prediction methods will bring the performance of the full closed-loop closer to that of the semiclosed-loop.

In future works, we will also explore the inversion of other metabolic models to design new inverse control algorithms, but the inversion of compartmental models is a complex task in which the complexity is inversely proportional to the model nonlinearity.

Acknowledgments

We especially acknowledge G. García-Sáez for her valuable contribution to this work. This research was partially financed by a Spanish FIS grant (ADVISING PI060437) and by a grant from the CIBER-BBN (PREDIRCAM 2008-09 CB06/01/0051).

Author Disclosure Statement

All authors declare no competing financial interests exist with any commercial associations in connection with the submitted article.

References

1. Hovorka R, Chassin LJ, Wilinska ME, Canonico V, Akwi JA, Federici MO, Massi-Benedetti M, Hutzli I, Zaugg C, Kaufmann H: Closing the loop: the Adicol experience. Diabetes Technol Ther 2004;6:307–318.
2. Clemens AH, Chang PH, Myers RW: The development of Biostator, a glucose controlled insulin infusion system (GCIIS). Horm Metab Res 1977;7:23–33.
3. Trajanoski Z, Wach P: Evaluation of subcutaneous route for closed-loop control of insulin delivery: numerical and experimental studies. Proc IEEE EMBS Conf 1995;45:1122–1134.
4. R. Bellazzi R, Nucci G, Cobelli C: The subcutaneous route to insulin dependent diabetes therapy. IEEE Eng Med Biol Mag 2001;20:54–64.
5. Carson ER, Deutsch T: A spectrum of approaches for controlling diabetes. IEEE Control Syst Mag 1992;12:25–31.
6. Naylor JS, Hodel AS, Morton B, Schumacher D: Automatic control issues in the development of an artificial pancreas. Proc Am Control Conf 1995;15:771–775.
7. Klonoff DC: The artificial pancreas: how sweet engineering will solve bitter problems. J Diabetes Sci Technol 2007;1:72–81.
8. Steil GM, Rebrin K, Darwin C, Hariri F, Saad MF: Feasibility of automating insulin delivery for the treatment of type 1 diabetes. Diabetes 2006;55:3344–3350.
9. Parker RS, Doyle FJ III, Peppas NA: A model-based algorithm for blood glucose control in type 1 diabetic patients. IEEE Trans Biomed Eng 1999;46:148–157.
10. Hovorka R, Canonico V, Chassin LJ, Haueter U, Massi-Benedetti M, Federici MO, Pieber TR, Schaller HC, Schaupp L, Vering T: Nonlinear model predictive control of glucose concentration in subjects with type 1 diabetes. Physiol Meas 2004;25:905–920.
11. Campos-Delgado DU, Femat R, Ruiz-Velazquez E, Gordillo-Moscoso A: Knowledge-based controllers for blood glucose regulation in type 1 diabetic patients by subcutaneous route. IEEE Int Intellig Control Symp 2003;30:592–597.
12. Kienitz KH, Yoneyama T: A robust controller for insulin pumps based on H-infinity theory. IEEE Trans Biomed Eng 1993;40:1133–1137.
13. Weinzimer SA, Dziura J, Steil GM, Kurtz N, Swan KL, Tamborlane WV: Fully automated closed-loop insulin delivery versus semiautomated hybrid control in pediatric patients with type 1 diabetes using an artificial pancreas. Diabetes Care 2008;31:5:934–939.
14. El-Khatib FH, Jiang J, Damiano ER: Adaptive closed-loop control provides blood-glucose regulation using dual subcutaneous insulin and glucagon infusion in diabetic swine. J Diabetes Sci Technol 2007;1:181–192.
15. Rodríguez-Herrero A, Hernando ME, Pérez-Gandía C, García-Saez G, Rigla M, de-Leiva A, Aguilera EJ: Adaptive inverse algorithm for closed-loop control in diabetes. In: 1st Conference on Advanced Technologies & Treatments for Diabetes. Kenes International, Prague, 2008, p. 46.
16. Bergman RN: Toward physiological understanding of glucose tolerance. Diabetes 1989;38:1512–1527.
17. Guyton RJ, Foster RO, Soeldner JS, Tan MH, Kahn CB, Koncz L, Gleason RE: A model of glucose-insulin homeostasis in man that incorporates the heterogeneous fast pool theory of pancreatic insulin release. Diabetes 1978;27:1027–1042.
18. Berger M, Rodbard D: Computer simulation of plasma insulin and glucose dynamics after subcutaneous insulin injection. Diabetes Care 1989:12:725–736.
19. Gómez-Aguilera EJ, Arredondo MT, Zoreda JL, del Pozo F: A simulator of therapies for education in diabetes. Proc IEEE EMBS Conf 1989;11:1965–1966.
20. Salzsieder E, Albrecht G, Fischer U, Rutscher A, Stephen RL, Stoewhas H: Assessment of individual pharmacokinetics and pharmacodynamics of insulin and its therapeutic consequences based on a model of the glucose-insulin system. Proc IEEE EMBS Conf 1990;12:1012–1014.
21. Lehmann ED, Deutsch T: A physiological model of glucose-insulin interaction in type 1 diabetes mellitus. J Biomed Eng 1992;14:235–242.
22. Hovorka R, Shojaee-Moradie F, Carroll PV, Chassin LJ, Gowrie IJ, Jackson NC, Tudor RS, Umpleby AM, Jones RH: Partitioning glucose distribution/transport, disposal, and endogenous production during IVGTT. Am J Physiol Endocrinol Metab 2002;282:992–1007.
23. Dalla Man C, Raimondo DM, Rizza RA, Cobelli C: GIM, simulation software of meal glucose–insulin model. J Diabetes Sci Technol 2007;1:323–330.
24. Neatpisarnvanit C, Boston JR: Estimation of plasma insulin from plasma glucose. IEEE Trans Biomed Eng 2002;49:1253–1259.
25. Kovatchev BP, Breton M, DallaMan C, Cobelli C: In silico preclinical trials: a proof of concept in closed-loop control of type 1 diabetes. J Diabetes Sci Technol 2009;3:44–55.

26. Wilinska ME, Chassin LJ, Schaller HC, Schaupp L, Pieber TR, Hovorka R: Insulin kinetics in type-1 diabetes: continuous and bolus delivery of rapid acting insulin. IEEE Trans Biomed Eng 2005;52:3–12.
27. Facchinetti A, Sparacino G, Zanderigo F, Cobelli C: Reconstructing by deconvolution plasma glucose from continuous glucose monitoring sensor data. Proc IEEE EMBS Conf 2006;28:55–58.
28. Eaton RP, Spencer W, Schade DS, Shafer BD, Corbett W: Diabetic glucose control: matching plasma insulin concentration to dietary and stress hyperglycemia. Diabetes Care 1978;1:40.
29. Breton MD, Shields DP, Kovatchev BP: Optimum subcutaneous glucose sampling and Fourier analysis of continuous glucose monitors. J Diabetes Sci Technol 2008;2:495–500.

Address correspondence to:
Agustín Rodríguez-Herrero, M.T.E.
Grupo de Bioingeniería y Telemedicina
ETSI Telecomunicación
Ciudad Universitaria s/n
28040 Madrid, Spain

E-mail: arodri@gbt.tfo.upm.es

This article has been cited by:

1. Roman Hovorka. 2011. Closed-loop insulin delivery: from bench to clinical practice. *Nature Reviews Endocrinology* . [CrossRef]
2. 2011. The 4th International Conference onAdvanced Technologies & Treatments for DiabetesLondon, UK/February 16–19, 2011The 4th International Conference onAdvanced Technologies & Treatments for DiabetesLondon, UK/February 16–19, 2011. *Diabetes Technology Therapeutics* **13**:2, 173-293. [Citation] [Full Text] [PDF] [PDF Plus]
3. 2010. Current literature in diabetes. *Diabetes/Metabolism Research and Reviews* **26**:5, i-x. [CrossRef]